JOURNAL OF AGRICULTURAL AND FOOD CHEMISTRY

Subscriber access provided by University of Wollongong Library

Agricultural and Environmental Chemistry

Synthesis of active strigolactone analogs based on eudesmane- and guaiane-type sesquiterpene lactones

Jesús G. Zorrilla, Antonio Cala, Carlos Rial, Francisco J. R. Mejías, José M. G. Molinillo, Rosa M. Varela, and Francisco A. Macías

J. Agric. Food Chem., **Just Accepted Manuscript** • DOI: 10.1021/acs.jafc.0c02361 • Publication Date (Web): 14 Aug 2020

Synthesis of active strigolactone analogs based on eudesmane- and guaiane-type sesquiterpene lactones

Jesús G. Zorrilla, Antonio Cala, Carlos Rial, Francisco J. R. Mejías, José M. G. Molinillo, Rosa M. Varela, Francisco A. Macías*

Allelopathy Group, Department of Organic Chemistry, Institute of Biomolecules (INBIO), Campus CEIA3, School of Science, University of Cadiz, C/ Republica Saharaui, 7, 11510-Puerto Real (Cádiz), Spain

ABSTRACT

Strigolactones are natural products that are exuded by plants and stimulate parasitic weed germination. Their use in herbicides is limited since they are produced in small quantities but the synthesis of bioactive analogs provides an alternative source. In this work eleven analogs have been synthesized. Among them, nine compounds belong to a novel family named eudesmanestrigolactones. The procedure is short (3–6 steps), the starting materials are isolated on a multigram scale and global yields are up to 8%, which significantly enhances isolated yields. In bioassay the compounds germinated high percentages of *Phelipanche ramosa*, *Orobanche cumana* and *Orobanche crenata* seeds, even at nanogram doses (100 nM). Bioactivity was stereochemistry-dependent and it is discussed in terms of the presence and geometry of the enol ether, orientation of the butenolide and unsaturation of ring A. The reported compounds provide a set of readily obtained allelochemicals with potential applications as preventive herbicides.

Keywords: sesquiterpene lactone, eudesmanolide, costunolide, dehydrocostuslactone, strigolactone analog, parasitic weed, *Orobanche*, *Phelipanche*.

INTRODUCTION

Phelipanche ramosa, *Orobanche cumana* and *Orobanche crenata* are holoparasitic broomrape species adapted to parasitize a broad range of cultivable plant species. *P. ramosa* can produce a significant decrease in the production of tomato, oilseed rape, buckwheat, tobacco and hemp crops. This weed is mainly located in Europe, North Africa and Western Asia but it has also been introduced in America and Australia and is the most widespread broomrape species.[1] *O. cumana* is a specific parasitic species for sunflower (*Helianthus annuus* L.) and it can produce serious yield losses for this source of seeds and oil.[2] *O. crenata* is the most damaging weed for temperate legumes around the Mediterranean basin and Middle East.[3] Just one single broomrape plant can disseminate thousands of seeds through wind and agricultural machinery due to the small size and weight of the seeds. In addition, parasitic seeds can remain dormant in soil for almost 20 years.[4] These parasitic species are a serious threat to agriculture and thus prevention is imperative.

The use of classical herbicides, based on compounds with long half-life, to control weed infestations raises severe issues with respect to the chemical properties. Some herbicides have proven to be effective, such as glyphosate or imidazolinones, but the new restrictions on their use in developed countries[5] limit their potential as a control strategy. Another disadvantage of classical herbicides comes from the high adaptability of parasitic weeds, with increasingly resistant populations after the use of agrochemicals that have a limited range of modes of action,[6] which reduces their effectiveness in the next season. Authorized specific herbicides may cause additional issues, e.g., the accumulation of toxic and carcinogenic residues in the soil and harvested products destined for human consumption.[7] The latter acquires special relevance as the demand for 'bio' products increases with time. Furthermore, some chemicals have been proven to accumulate for decades in the soil, such as pesticides based on chlorinated hydrocarbons.[8]

The strategy known as 'suicidal germination', which is also called the 'honeypot strategy', enables the prevention of parasitic weed infestations. This strategy requires the use of specific compounds that are chemically recognizable by parasitic seeds and are applied to the soil

before sowing, thus triggering germination in the absence of host plants and ultimately leading to the death of obligate parasites by starvation after few days.[9]

Strigolactones are known as a family of natural products that stimulate the germination of parasitic *Orobanche* and *Phelipanche* seeds in nature, and they are exuded by host plants.[10] These compounds act as phytohormones and they are involved in the regulation of development processes like shoot branching, they act as phytohormones.[11] The structure of strigolactones is related to that of strigol (*figure 1*).

However, natural strigolactones are not useful for the formulation of agrochemicals based on suicidal germination since their isolation from natural sources gives low yields (isolation of several micrograms requires thousands of plants)[12] and their high degree of chirality requires a complex total synthesis with multiple steps. Strigolactone analogs are designed to simplify the synthesis of these germination elicitors and this approach is based on the semisynthesis from structurally related natural products that can be obtained on a multigram scale from natural sources. The search for new bioactive strigolactone analogs is a hot topic that is being investigated by numerous research groups around the world.[13–16] The main aim of the study reported here was to achieve the efficient synthesis of strigolactone analogs.

Sesquiterpene lactones share structural similarities with strigolactones and can stimulate the germination of parasitic weed seeds. Lactones costunolide (**1**) and dehydrocostuslactone (**5**) (*figure 2*) can be isolated on a multigram scale from an extract of *Saussurea costus* and these were reported to be the main compounds responsible for parasitic recognition of sunflower by *O. cumana*.[17] Since these compounds possess a lactone moiety (C-ring in strigolactones), the addition of an extra butenolide ring connected by an enol ether bond to **1** and **5** allows strigolactone analogs to be obtained.[18]

The main objective of the work reported here was the preparation of new strigolactone analogs by the addition of the butenolide ring to the hydroxylated derivatives of **2**, **3**, **8** (*figure 2a*) and **5** (*figure 2c*). This is the first time that strigolactone analogs based on eudesmanolides

have been reported. All of the strigolactone analogs were tested in a parasitic seed germination bioassay in order to evaluate their potential use as preventive agrochemicals for broomrape control. *P. ramosa*, *O. cumana* and *O. crenata* were the species chosen for testing to identify the most promising products for the preparation of pre-emergency herbicides through the honeypot strategy. The likely structure-activity relationships (SAR) are also discussed.

MATERIALS AND METHODS

General Experimental Procedures. The purity of each compound was assessed by ^{1}H NMR spectroscopy prior to the bioactivity tests. The structural determination of all compounds was carried out by combining 1D- (^{1}H, ^{13}C) and 2D-NMR (^{1}H-^{1}H COSY, NOESY, ^{1}H-^{13}C HSQC and HMBC) experiments along with specific rotation, UV, FTIR and, in particular, MS to determine the molecular formulae. ^{1}H NMR and ^{13}C NMR spectra were recorded on Agilent spectrometers at 400 and 500 MHz using $CDCl_3$ (MagniSolv™, Merck) as solvent. The residual solvent peaks were used as internal reference (δ 7.26 ppm in ^{1}H and δ 77.0 ppm in ^{13}C NMR for $CDCl_3$). COSY, HSQC, HMBC and NOESY experiments were performed using Varian vnmrj microprograms. Exact masses were measured on a UPLC-QTOF ESI (Waters Synapt G2, Manchester, UK) high-resolution mass spectrometer (HRTOFESIMS). Mass spectra were recorded in the negative- or positive-ion mode in the range *m/z* 100–2000, with a mass resolution of 20,000 and an acceleration voltage of 0.7 kV. FTIR spectra were obtained on Perkin–Elmer Spectrum TWO IR spectrophotometer. Major absorptions in the infrared are given as wavenumbers ῡ in cm^{-1}. Optical rotations were measured in $CHCl_3$ on a JASCO P-2000 polarimeter.

Column chromatography (CC) was performed on silica gel (Merck, Geduran® Si 60, 0.063–0.200 mm). The reagents and HPLC quality solvents were supplied by either Sigma-Aldrich Co. (St. Louis, Missouri), Merck (Darmstadt, Germany) or Alfa Aesar (Ward Hill, Massachusetts). HPLC was carried out on a Merck-Hitachi D-7000 system (Tokyo, Japan) with a refractive index detector (Elite LaChrom L-2490). A semipreparative LiChrospher 250–10 Si

60 (10 μm) column (Merck) and an analytical LiChroCART 250-4 Si 60 (5 μm) column (Merck) were employed with a flow rate of 3 mL/min and 1 mL/min, respectively.

Synthesis of derivatives. Strigolactone analogs were synthetized from eudesmanolides **2**, **3** and **8**, and guaianolide **5** (*figure 2*). The starting materials **1** and **5** were isolated from a natural source, i.e., a *Saussurea costus* root extract, and eudesmanolides **2** and **3** were obtained by reaction of **1** under acidic conditions following the procedure reported in the literature,[19] while eudesmanolide **8** was synthetized from compound **3** (*figure 2a*). The structures of eudesmanolides **2**–**4** were confirmed by comparison of the experimental data with those reported in the literature.[20, 21] The ^{1}H and ^{13}C NMR spectra for **2** were included in our previous study, and spectra and experimental NMR data for compounds **3** and **4** are included in the supporting information for completeness.

Synthesis of eudesmanolide 8. Following the procedure reported previously for santamarine,[22] compound **3** (0.15 mmol) was treated with excess (0.75 mmol) 2,3-dichloro-5,6-dicyano-1,4-benzoquinone (DDQ) in CH_2Cl_2 under reflux (24 h) to obtain **8** in 67% yield. The structure of **8** was confirmed by comparing the ^{1}H and ^{13}C NMR spectra with those reported for 3-deoxybrachylaenolide[23] and these are included in the supporting information for completeness.

Synthesis of alcohols 7, 12, 13 and 14. The two-step synthetic procedure reported to obtain alcohols **7** and **12** (*figures 2a* and *2c*), i.e., Michael addition of 3-methoxybenzyl alcohol and subsequent oxidation with DDQ, was applied to obtain **7** and **12**, and also to transform **3** and **8** into the new ethers **10** (42%) and **11** (40%), respectively, and then into the new alcohols **13** (86%) and **14** (87%), respectively. This procedure was applied in a previous study to obtain **12** from **2**[19] and the yield for the second step was improved from 62% to 75% by carrying out the reaction of **9** with DDQ without water. The spectra and experimental data for new compounds are provided in the supporting information.

Synthesis of aldehydes 15, 16 and 17. Compound **12** (47.5 mg, 0.19 mmol) was dissolved in CH_2Cl_2 (5 mL) and added to a round-bottomed flask containing Dess–Martin

periodinane (67.6 mg, 0.27 mmol). The mixture was stirred for 3 h at room temperature, quenched with saturated aqueous $NaHCO_3$ (10 ml) and extracted with EtOAc (3 × 10 ml). The combined organic layers were washed with brine and dried over anhydrous Na_2SO_4. The solvent was evaporated under vacuum to obtain a crude product, which was purified by column chromatography with a gradient of 1:0−3:2 *n*-hexane:EtOAc to give 30.1 mg of **15** (61% yield). The same procedure was carried out on **13** and **14** to obtain **16** and **17** in 62% and 55% yield, respectively. The spectra and experimental data for new compounds are provided in the supporting information.

Synthesis of eudesmanestrigolactones (EDSLs) 18–26. The addition of the butenolide fragment to aldehydes **15**–**17** was carried out using (±)-5-bromo-3-methyl-2(5*H*)-furanone, which was synthesized according to the previously described method.[24] Compound **15** (50.0 mg, 0.2 mmol) was added to a dry round-bottomed flask containing tetrahydrofuran (THF) (2 mL) under Ar and potassium *tert*-butoxide (0.2 mL of a 1.0 M solution in *tert*-butanol, 0.2 mmol) was introduced with cooling (ice bath) and the mixture was stirred for 10 min. Freshly synthesized (±)-5-bromo-3-methyl-2(5*H*)-furanone (0.8 mmol) was added and the reaction mixture was stirred for 1 h. Water (1 mL) was added and the product was extracted (×3) with EtOAc (5 mL) and dried over anhydrous Mg_2SO_4. The solvent was evaporated under vacuum to give a crude product, which was purified by column chromatography with a gradient of 1:0−3:2 *n*-hexane:EtOAc. Mixtures of epimers **18**–**19** and **20**–**21** were collected and then purified by HPLC on a Merck Hitachi D-7000 HPLC system in isocratic mode equipped with a semipreparative LiChroCART 250-10 Si 60 (10 μm) column, using *n*-hexane:EtOAc 3:2 as eluent. Yields for isolated epimers were 16% (**18**), 24% (**19**), 6% (**20**) and 5% (**21**).

Aldehydes **16** and **17** were treated under the same conditions as aldehyde **15**. The reaction of **16** let to obtain products **22** (mixture of epimers) and **23** in 38% and 9% yield, respectively; while reaction of **17** let to obtain products **24** and **25** in 6% and 10% yield, respectively. Evidence for the formation of the epimer of **23**, **24** or **25** was not observed during the synthetic and chromatographic procedures. Once obtained the target EDSLs (**18-25**), the butenolide fragment

was added to the alcohol **12** by using the same conditions, to give dihydro-EDSL **26** (*figure 2a*) in 54% yield. Evidence for the formation of the epimer of **26** was not observed during the synthetic and chromatographic procedures. The spectra and experimental data for new compounds are provided in the supporting information.

Synthesis of dihydroguaianestrigolactones (27–28). Compound **7** (75 mg, 0.300 mmol) was dissolved in THF (1 mL) under an Ar atmosphere (*figure 2c*). The solution was added to a round-bottomed flask containing NaH (21.6 mg, 3 eq) under Ar with cooling (ice bath), The mixture was stirred for 10 min. A solution of freshly synthesized (±)-5-bromo-3-methyl-2(5*H*)-furanone in dry THF (2 mL) was added (1.2 mmol) and the mixture was stirred for 64 h. The reaction was quenched with saturated aqueous NH_4Cl (20 mL) and the aqueous layer was extracted with EtOAc (3 × 20 mL). The combined organic layers were dried over anhydrous Na_2SO_4 and the solvent was evaporated under vacuum to obtain a crude product, which was purified by column chromatography with a gradient of *n*-hexane/EtOAc 4:1–3:2 as eluent. Three major fractions were obtained as follows: 31 mg of the mixture of epimers **27** and **28** (30%), 28 mg of recovered **7** (37%) and, unexpectedly, 29 mg of compound **29** (16%).

The epimeric mixture of **27** and **28** was separated on a Merck Hitachi D-7000 HPLC system in isocratic mode equipped with an analytical LiChroCART 250-4 Si 60 (5 μm) column and a mixture of *n*-hexane:$(CH_3)_2CO$ 85:15 as eluent. The dimer **29** was purified using the same HPLC system equipped with a semipreparative LiChroCART 250-10 Si 60 (10 μm) column, using *n*-hexane:EtOAc 14:6 as eluent. Injections of 0.10–0.20 mg had to be carried out in order to avoid coelution of the compounds due to the similarity in the polarity of the two compounds. Spectra and experimental data for **27**–**29** are provided in the supporting information.

Circular dichroism experiments. In order to identify the absolute stereochemistry of compounds **18**–**21** and **23**–**28**, each compound was dissolved in MeOH and the spectra were obtained on a JASCO J-1500 instrument (*figure 3*). The theoretical ECD were obtained using Gaussian 16 with B3LYP/6-311g (d,p) optimized geometries. In each case, the polarizable continuum model with methanol was employed to obtain accurate theoretical CD spectra. The

conformers employed were minimum energy, also obtained with B3LYP/6-311g (d,p). The absolute configuration was determined by circular dichroism by comparison of the theoretical calculations with experimental data.

Bioassay. The strigolactone analogs **18**–**28**, as well as the dimeric byproduct **29**, were tested in the broomrape seed germination bioassay on three species, namely *Orobanche cumana*, *Orobanche crenata* and *Phelipanche ramosa*, in the concentration range 10^{-4}–10^{-7} M. The most active compounds (**19** and **24** for *O. cumana* and **20**, **21**, **23**, **24**, **28** and **29** for *P. ramosa*) were tested in the concentration range 10^{-4}–10^{-12} M to obtain full inhibition curves. The synthetic compound GR24 was included as a positive control for the broomrape bioassay and deionized sterilized water with 1% v/v acetone was used as a negative control, where spontaneous germination was not observed.

The procedure for the bioassay has been reported previously[19] and it is included in the supporting information. Seeds of *O. Cumana* were provided by Dr. Leonardo Velasco (Instituto de Agricultura Sostenible, CSIC, University of Cordoba, Spain) and seeds of *O. crenata* and *P. ramosa* were provided by Dr. Maurizio Vurro (Institute of Sciences of Food Production, National Council of Research, Bari, Italy).

Calculation of EC_{50} values. The compounds that gave minimum activities of 50% and were active at more than one concentration were statistically analyzed for their EC_{50} value using the GraphPad Prism v.5.00 software package (GraphPad Software, Inc., San Diego, USA). The bioactivity data were fitted to a sigmoidal dose-response model with constant slope. The results of this analysis are shown in *table 1*.

RESULTS AND DISCUSSION

Eudesmanolides **2**, **3** and **8** (*figure 2a*) were chosen as targets for the synthesis of novel strigolactone analogs named eudesmanestrigolactones (EDSLs). Compounds **2** and **3** were obtained by cyclization of costunolide (**1**), a germacrane-type sesquiterpene lactone isolated together with compound **5** in gram scale from *Saussurea costus* roots. Compound **8** was also

209 considered as it is an affordable eudesmanolide obtained by reaction of **3** with excess DDQ. The
210 method presented herein to obtain **8** from α-cyclocostunolide (**3**) is reported for the first time.

211 Our recent results demonstrated that compound **2** stimulates germination of *O. cumana*
212 and *P. ramosa* seeds significantly (significance level of 0.05), with EC_{50} values of $7.31 \cdot 10^{-6}$ M
213 and $<10^{-7}$ M, respectively,[19] but other studies were not found in the literature regarding
214 strigolactone analogs based on eudesmanolides. However, strigolactone analogs based on **5** were
215 designed and tested previously and promising results were obtained.[4]

216 Analogs were synthesized by adding a butenolide ring to the hydroxylated derivatives at
217 C-13 of **2**, **3**, **8** (EDSLs, *figure 2a*) and **5** (dihydro-GELs, *figure 2c*). These alcohols (compounds
218 **12-14** and **7**) were synthesized in two steps from the starting eudesmanolide (**2**, **3** or
219 **8**)/guaianolide (**5**), and the procedure to add the butenolide ring required the prior formation of
220 aldehydes at C-13 (**15-17**) to achieve strigolactones with an enol ether bond (**18-25**).

221 A previous strategy involved hydroxylation at C-13 with the use of
222 hexamethylphosphoramide (a highly toxic reagent), long reaction time (5 days) and high
223 temperature (80 ºC), and it produced an undesired dihydroxylated byproduct.[4] As reported
224 recently, we succeeded in hydroxylating **2** and **5** in two steps by Michael addition of 4-
225 methoxybenzyl alcohol at C-13 followed by oxidation with DDQ, with high yields obtained for
226 both target compounds **12** (71%) and **7** (54%).[19] In the present study, this procedure was improved
227 and applied to compounds **3** and **8** for the first time to obtain ethers **10** and **11**, and then alcohols
228 **13** and **14**, respectively. Furthermore, the yield for the formation of **12** was improved.

229 **Synthesis of ethers and 13-hydroxy derivatives.** The Michael addition of 4-
230 methoxybenzyl alcohol to C-13 of **3** and **8** was successfully proceeded to give ethers **10** and **11**
231 in 42% and 40% yield, respectively (*figure 2a*). Ethers **6** (63%) and **9** (46%) were synthesized in
232 our previous work by following the same procedure and the spectroscopic data were consistent
233 with literature data.[19] In a similar way to compound **9**, the ^{1}H NMR spectra of products **10** and **11**
234 showed a new signal for H-11 at δ 2.49 and δ 2.53, respectively, and these correlated with C-11

at δ 46.6 and δ 46.9 in the ^{13}C NMR spectra. These signals match with sp^2 signals that are absent in compounds **3** and **8**. Furthermore, signals for H-13 in the ^{1}H NMR spectra in both cases were shifted from lower field to higher field when compared with **3** (from δ 6.06 and δ 5.38 to δ 3.77 and δ 3.71) and **8** (from δ 6.10 and δ 5.42 to δ 3.78 and δ 3.72). The new ^{1}H signals at δ 7.24 and δ 6.88 (corresponding to a benzyl ring disubstituted in the *para*-positions), as well as the new signal at δ 3.80, confirmed the presence of the methoxybenzyl moiety in **10** and **11**. Coupling constant value between 12.6 and 12.8 Hz between H-7 and H-11 confirmed the stereochemistry of the compounds. The ^{13}C signals were assigned with each of their ^{1}H signals and the position in the molecule was identified by correlations observed in the 2D NMR experiments.

Following the procedure reported to obtain alcohols **7** and **12**, compounds **10** and **11** were subsequently oxidized using DDQ to give alcohols **13** and **14** in 86% and 87% yield, respectively (*figure 2a*). As in the case of the ethers, the NMR spectra of new products (**13** and **14**) were very similar to those of previously synthetized **12**. The loss of the methoxybenzyl moiety was evidenced by the absence of aromatic and methoxy signals in the spectra of **13** and **14,** when compared with the spectra of ethers **10** and **11**. Furthermore, H-13 signals were shifted to lower field, from δ 3.77 and δ 3.71 to δ 3.97 and δ 3.78 in the case of **13**, and from δ 3.78 and δ 3.72 to δ 3.99 and δ 3.80 in the case of **14**. The FTIR spectra showed a broad band at 3450 cm^{-1} and this indicates the presence of a hydroxyl group in the molecule. Once again, coupling constant values between 12.8 and 13.0 Hz between H-7 and H-11 confirmed the stereochemistry of the compounds. ^{13}C signals were assigned with related ^{1}H signals and the positions in the molecule were identified by correlations observed in the 2D NMR experiments.

Synthesis of aldehydes. The eudesmanolide alcohols **12**–**14** were oxidized to the corresponding aldehydes prior to the addition of the butenolide ring to obtain the strigolactone analogs (*figure 2a*). Primary alcohols are typically oxidized to aldehydes under mild conditions with Dess–Martin periodinane.[25] The aldehydes resulting from the oxidation of the eudesmane alcohols (**12**, **13**, **14**) are reported herein for the first time, with yields of 61%, 62% and 55% obtained for **15**, **16** and **17**, respectively.

Success in the synthesis of **15**–**17** was verified by the ^{1}H NMR spectra after observing a new signal centered at δ 9.87, which is typical of an aldehyde and was assigned to H-13. A new signal at δ 196.0 in the ^{13}C NMR spectra, assigned to C-13 by correlations observed in the 2D NMR experiments, confirmed the presence of an aldehyde group.

Synthesis of strigolactone analogs. A total of nine EDSLs were synthesized from the aldehydes **15**–**17** (EDSLs **18**–**25**) and alcohol **12** (EDSL **26**) (figure 2b). This last step required the formation of the enolate of the starting aldehyde/alcohol by reaction with potassium *tert*-butoxide. Then, four equivalents of brominated furanone (a compound with low stability that was obtained immediately prior to use)[24] were added (*figure 2a*). A nucleophilic substitution was carried out in which the nucleophlilc oxygen of the enolate bonds with the furanone, forming EDSLs **18-26** and KBr precipitated as consequence.

Reaction of aldehyde **15** gave four isolated EDSLs (**18**–**21**) after column chromatography and HPLC purification of the crude products. Confirmation of the isolation of pure epimers was evidenced by NMR spectroscopy, since prior to HPLC separation, the spectra showed duplicated signals. When these fractions were purified, two different peaks were collected from each fraction, and NMR spectra of each peak showed that signals were not duplicated. Since the starting material (**1**) was enantiomerically pure, these compounds should also be pure enantiomers. The yields obtained were 15% (**18**), 23% (**19**) and 5% (**20** and **21**). The molecular formulae determined by MS ($C_{20}H_{24}O_5$) were consistent with the target compounds. The ^{1}H and ^{13}C NMR spectra of the compounds showed the signals corresponding to the newly introduced butenolide ring: H-2' (δ 6.08), H-3' (between δ 6.90 and δ 6.87) and H-1" (between δ 2.00 and δ 1.95). The presence of the C-11–C-13 double bond that forms the enol ether was evidenced in the ^{1}H NMR by the absence of a signal for H-11 and by the new shift of H-13, which changed from δ 9.86 to δ 7.36 (**18**), δ 7.35 (**19**), δ 6.50 (**20**) and δ 6.51 (**21**). NOESY1D experiments were used to assign the geometry of the double bond, where H-13 of **18**–**19** showed an NOE effect with H-7, thus evidencing their proximity in space and, therefore, the 11*Z* geometry (*figure 3*).

Compounds **20**–**21** were identified as 11*E* stereoisomers. The yields for 11*Z* products (38%) were higher than those for 11*E* products (10%).

Absolute configuration was determined by experimental and theoretical ECD spectra for EDSLs (*figure 4a*) and the stereochemistry of C-2′ and C-11 was determined by comparison with the experimental values.

EDSL **19** showed two bands at 210 nm and 225 nm with a sign change in the rotation angle – in contrast to **18**, which showed the same two bands at positive angles, albeit with a bathochromic effect. According to the differences between **18** and **19**, the *R* and *S* configuration at C-2′ is excited in the range 225–240 nm. In this case, the total configurations can be assigned as $\Delta^{4,15}$-(11*Z*)-(2′*R*)-eudesmanestrigolactone (**18**) and $\Delta^{4,15}$-(11*Z*)-(2′*S*)-eudesmanestrigolactone (**19**). Epimers **20** and **21** showed the same maximum absorption band as their *Z* counterparts (**18** and **19**), but differences between their ECD were more pronounced. Changes from positive to negative angles are displayed in **21** but just one positive band at 225 nm was observed for **20**, with this curve having the best fit in theoretical calculations. According to the calculated spectra, assignment becomes easy between these epimers, where $\Delta^{4,15}$-11*E*-2′*R*- eudesmanestrigolactone corresponds to **20** and $\Delta^{4,15}$-11*E*-2′*S*-eudesmanestrigolactone corresponds to **21**.

Reaction of aldehydes **16** and **17** let to obtain two EDSLs from each aldehyde, namely compounds **22**–**23** and **24**–**25**, respectively. Authors suggest that all possible epimers were synthetized, but those with lowest yields could not be detected during the chromatographic purification procedures. Similar structural elucidation was carried out as in the cases of **18**–**21**.

Compound **22** was obtained in 38% yield as a mixture of epimers at C-2' (evidenced by the duplicity of signals at NMR spectra) but the purification of these epimers by HPLC was proved to be difficult. However, this compound was considered to be 11*Z* due to the NOE effect observed between H-13 and H-7 (*figure 3*). Compound **23** was obtained in 9% yield and was assigned as the 11*E* counterpart. It is noteworthy that the higher yield obtained in the synthesis of 11*Z* compounds (**22**) also occurred with EDSLs **18**–**21**. Regarding the absolute configuration of

23, the experimental circular dichroism spectrum showed a negative band at 230 nm after the rise of a positive band at 210 nm. This fingerprint is consistent with (11*E*)-(C-2'*R*)-EDSL as it is opposite to the calculated ECD spectrum of (11*E*)-(C-2'*S*)-EDSL (*figure 4a*).

EDSLs **24** and **25**, both obtained by reaction of **17** in 5% and 9% yield, respectively, were submitted to theoretical ECD. The results show that the *R*-epimers were selectively synthesized. The experimental spectrum of **24** showed two maximum positive absorption bands at 205 nm and 230 nm and these are consistent with the calculated spectrum for $\Delta^{1,2},\Delta^{4,15}$-(11*Z*)-(2'*R*)-EDSL. In the case of **25**, only one high positive band appeared at 235 nm, similar to that found in the calculated spectrum of $\Delta^{1,2},\Delta^{4,15}$-(11*E*)-(2'*R*)-EDSL with a bathochromic effect.

In order to complete the study and compare the effect of the absence of C-11–C-13 double on the activity, the 11,13-dihydro-EDSL **26** was synthesized by directly adding the butenolide fragment to alcohol **12**. The reaction conditions were the same as those used for the synthesis of EDSLs **18**–**25** (*figure 2a*). Thus, **12** was treated with potassium *tert*-butoxide and brominated furanone to give **26** in 54% yield.

The NMR spectra of **26** were very similar to those of previous EDSLs, with the same pattern for the butenolide fragment and changes specifically for H-13 and C-13. In the absence of the double bond, the H-13 signal shifted to higher field and was observed as two *dd* at δ 3.96 and δ 3.79 – in contrast with EDSLs, where it appeared between δ 7.39 and δ 6.49. The lack of a double bond is also evidenced by the additional signal for H-11 (δ 2.53), which is absent for EDSLs **18**–**25**. An NOE effect between H-11 and H-6 confirmed the 11*R* stereochemistry of **26** (*figure 3*), while the absolute stereochemistry at C-2′ was analyzed by ECD. The experimental spectrum showed a positive band at 220 nm and a negative band at 280 nm, which are consistent with the C-2'*R* epimer rather than the C-2'*S* epimer, which showed opposite degrees (*figure 4b*). The epimer at C-2′ was not observed in this reaction. This result suggests that the C-*2'S* addition of the butenolide ring is highly impeded by steric effects.

In addition to EDSLs, in this study the butenolide ring was added to compound **7** and the epimers were purified and evaluated separately for the first time (*figure 2c*), since the epimers at C-2', i.e., mixture of **27**+**28**, obtained from **7** were previously found to be bioactive.[4] A solution of **7** in dry THF was added to a dry round-bottomed flask with cooling (ice bath) and the brominated furanone (4 equivalents) was added. The base NaH (3 equivalents) was added. Compounds **27**+**28** were obtained (30%) along with the unexpected byproduct **29** (16%) and unreacted starting material **7** (37%).

In an effort to improve the yields of **27**–**28**, the use of other bases than NaH was evaluated but none of them showed to be more favorable. On using KH a yield of 13% was obtained for the mixture **27**+**28**, 4% for the mixture of their epimers at C-11 and 60% recovered starting material. On using the aforementioned conditions and treating **7** with BuLi, dimer **29** was obtained in 6% yield and **27** or **28** were not observed. Since only NaH provided the target compounds in good yields, the authors suggest that the size of the counterion ($K^+ > Na^+ > Li^+$) could hinder the reaction, and the size of Na^+ encourage the reaction pathway.

The ^1H and ^{13}C NMR spectra of each epimer were similar to those of the mixture reported in the literature, with the exception of H-13, which gave a multiplet at δ 4.10 for **27** and two well-resolved *dd* at δ 3.98 and δ 3.86 for **28**. The bonding of the butenolide ring was evidenced by the presence of signals for H-2' (δ 5.84 for **27** and δ 5.89 for **28**), H-3' (δ 6.81 for **27** and δ 6.86 for **28**) and H-1" (δ 1.95 for **27** and δ 1.97 for **28**), which are similar to those in the ^1H NMR spectra of **18**–**26** but are absent from the spectrum of **7**.

The absolute configuration of C-2' was determined by electronic circular dichroism. The experimental ECD spectrum of **27** showed a negative minimum at 243 nm and a positive maximum at 212 nm, while **28** gave a positive maximum at 245 nm and a negative minimum at 205 nm. These experimental results are in agreement with the theoretical spectra and **27** was assigned as C-2'*S* while **28** corresponded to the C-2'*R* epimer (*figure 4b*).

Finally, spectroscopic analysis of the unexpected product **29** confirmed that this was an ester of **7**, which might be formed by the opening of the butenolide ring after the nucleophilic substitution due to the strongly basic conditions used. The molecular formula determined by MS was $C_{35}H_{42}O_8$ and this corresponds to the dimeric compound **29**. In the ^{1}H NMR spectrum, a quartet at δ 5.88 (vinyl proton, H-17) and a doublet at δ 2.08 (H-20) indicated the formation of a dimer. Two major clues were obtained on analyzing the ^{13}C spectrum: there were two extra signals for carbonyl groups when compared with **7** (δ 164.4 and δ 168.4) and almost all of the signals were duplicated when compared with the original compound, with the exception of the following: δ 164.4 (C-16), δ 120.2 (C-17), δ 146.3 (C-18), δ 168.4 (C-19), δ 20.7 (C-20), all of which were new signals. All of these signals corresponded to the new linear chain connected to C-13. After a careful analysis of the ^{1}H NMR signals, it was found that most of them were two overlapping signals that integrated for double the value of the similar signals of **7**. Finally, an NOE effect was observed between H-17 (δ 5.87) and H-20 (δ 2.07), which evidenced their proximity in space and confirmed the *Z* configuration of the C-17–C-18 double bond (*figure 3*), thus confirming the structure of compound **29**.

Broomrape seed germination bioassay. The synthesized strigolactone analogs (**18**–**28**) and the dimer **29** were tested in the broomrape seed germination bioassay, which evaluates the ability of compounds to stimulate the germination of parasitic plant seeds. The species tested were *P. ramosa*, *O. cumana* and *O. crenata*. Synthetic strigolactone GR24 (*figure 1*) was used as a positive control and deionized sterile water with 1% v/v acetone was used as a negative control. GR24 has a high germinating activity on seeds of these three species and it is widely used as a reference control in this area of research.[26] The main goal of this bioassay was to obtain information in order to select the best candidates for the design of agrochemicals to treat broomrape infestations on crops through the honeypot strategy. The results are represented in *figure 5* for a range of concentrations from 10^{-4} M to the minimum significant dose of each compound (up to 10^{-10} M), as the mean percentage of seeds that germinated in each plate. The negative control did not cause significant spontaneous germination.

All of the compounds tested were active on *P. ramosa* and *O. cumana* and the EDSLs **18**–**20** and **22**–**25** were also significantly active on *O. crenata*.

The profiles of all of the tested compounds showed significant activity at all concentrations tested on *P. ramosa* (*figure 5*). At the highest concentration, **20**, **21**, **23**–**26**, **28** and **29** stimulated the germination of more than 80% of seeds, with percentages of 100% achieved in some cases. Compounds **20**, **21**, **23**, **24**, **28** and **29** are noteworthy since the activity levels were retained at the lowest concentrations and were even higher than that of the positive control GR24. Calculation of the EC_{50} gave values of less than 10^{-7} M (*table 1*). Thus, these last readily obtained compounds could be great agrochemicals to prevent *P. ramosa* pests, being a better option than GR24 in terms of obtaining or activity levels.

From a structural point of view regarding *Z*/*E* configuration, better stimulation was provided by 11*E*-EDSLs (**20**, **21** and **23**) when compared with 11*Z*-EDSLs (**18**, **19** and **22**) on *P. ramosa* seeds, with differences as great as 60% of seed germination. In the case of EDSLs with two double bonds at ring A (**24** and **25**), the 11*E* stereoisomer (**25**) had slightly lower activity at the two lowest concentrations, while **24** retained a high 77% activity at 10^{-7} M.

On comparing stereochemistry at C-2', compound **28** (C-2'*R*), which has the same stereochemistry as strigol, was more active than its epimer **27** (C-2'*S*). Significant differences were not observed in the cases of EDSLs **18**–**21**. Regarding the presence of an enol ether bond, the absence of a double bond between C-11 and C-13 did not seem to have a significant effect (see **18**–**21** vs **26**), as **26** reached 98% germination at the highest concentration, although this percentage decreased rapidly at lower concentrations.

All of the compounds stimulated the germination of *O. cumana* seeds. In particular, EDSLs **18**–**26** were highly effective in stimulating seeds of this problematic species, with stimulation values over 90% for most of the higher concentrations. At 10^{-5} M, all EDSL analogs (**18**–**26**) reached at least 70% germination. Their profiles are similar or even better than that of GR24, so these readily obtained strigolactone analogs could be great agrochemicals to prevent *O.*

417 *cumana* pests, being a better option than GR24 in terms of obtaining or activity levels. Especially,
418 compounds **19** and **24** retained stimulatory activity even at lower doses, with 78% and 85%
419 germinated seeds respectively at 10^{-7} M and significant activity at 10^{-8} M, so both could be the
420 most suitable agrochemical compounds, as they can be applied at lower doses, reducing the
421 environmental impact. Germination was not detected for **25** at the highest concentration, while
422 values over 90% were observed at 10^{-5} M. This phenomenom has been observed previously[19] and
423 can be explained by the phytotoxicicity of **25** on *O. cumana* at high doses (*figures 5* and *6*).
424 Dihydro-GELs (**27**–**28**) and, in particular, the dimer **29** also showed significant activity at the two
425 highest concentrations.

426 Regarding the stereochemistry of the enol ether bond, the opposite trend to *P. ramosa*
427 was found in *O. cumana*, with the 11*Z*-EDSLs (**18**, **19**, **22**, **24**) being more active than the 11*E*-
428 EDSL (**20**, **21**, **23**, **25**) stereoisomers, especially at lower concentrations. As far as the orientation
429 of C-2' is concerned, the profiles for **18**–**21** show that the C-2'*S* orientation (**19** and **21**) is better
430 than *R* (**18** and **20**), especially at the lowest concentrations. In fact, compound **19** retained a value
431 of 78% activity at 10^{-7} M, while its epimer **18** gave a value of only 43%. Significant differences
432 were not observed between the two dihydro-GEL epimers (**27**–**28**), although their activity levels
433 were lower than those of the EDSLs tested. Regarding the enol ether bond, the absence of a double
434 bond (**26**) did not lead to a significant activity decrease when compared with compounds **18**–**21**.

435 Seeds of *O. crenata* have proven to be highly selective to compounds that stimulate their
436 germination, as null or very low percentages of germinated seeds were obtained in previous
437 studies.[22,24,27]

438 The results presented in *figure 5* show that nearly all EDSLs (**18**–**26**) stimulated
439 germination of *O. crenata* significantly at the highest concentration. It is worth highlighting
440 compounds **22** and **25** as these are the only examples that showed significant activity at 10^{-5} M
441 (47 and 45%, respectively). Compounds **26**–**29**, which lack the C-11–C-13 double bond,
442 presented null germination for this species, thus demonstrating the critical role of the enol ether
443 system in the mechanisms involved in this parasite recognition for germination. The *Z*/*E*

conformation of the enol ether bond, as well as the *R*/*S* orientation of C-2', did not appear to be critical factors to generate significant differences in activity profiles, whereas unsaturation of ring A led to an improvement in activity in the cases of **22** and **25**, which are derivatives of **3** and **8**, respectively, when compared with **18**–**21**, which are derivatives of **2**.

Finally, the activity of EDSLs (*figures 2b*) will be compared with three of the most relevant natural strigolactones that are germination stimulants, namely strigol, orobanchol and sorgolactone.[28] The enol ether bond in these molecules has an *E* geometry and the configuration of C-2' is *R*. Thus, it is reasonable to consider that the most active compounds would have these isomeric features. The molecules studied in the bioassay reported herein allowed us to evaluate whether different isomerism to that of natural strigolactones would provide a higher stimulation activity on seed germination. EDSLs **20** and **25** have the same stereochemistry as natural strigolactones. For *P. ramosa*, compound **20** was the most active of the EDSLs synthesized from β-cyclocostunolide (**18**–**21**), which verifies the aforementioned hypothesis. However, unsaturation at ring-A seems to play a key role, as compound **24** shows higher activity than its stereoisomer **25**. EDSLs **20** and **25** are the most active compounds for *O. cumana* at the highest concentration tested when compared with the molecules with which they share the same ring-A, with the additional advantage that **25** shows a phytotoxic effect. It is remarkable that **19**, which has the opposite stereochemistry to the natural strigolactones, is one of the most active compounds tested. In the case of *O. crenata*, compound **25** has an improved profile when compared to its analog **24**. However, compound **20** showed very similar results to **18** and **19**. Thus, it has been shown that alternative stereochemical features when compared to natural strigolactones are also capable of generating similar profiles for *O. crenata* germination.

The activity profiles from the bioassay led us to conclude that different structural features can give better results depending on the parasitic species: on *P. ramosa* and *O. cumana* the stereochemistry of the enol ether bond explains differences in activity, while *O. cumana* profiles were also affected by the presence of eudesmanolide or guaianolide structures, with better profiles obtained for eudesmanolide derivatives. In the case of *O. crenata*, the lack of an enol ether bond

in the strigolactone analogs led to the total absence of activity. The unsaturation at ring A of EDSLs affected the activity for the three species tested. The best compounds to stimulate the germination of *P. ramosa* are **20**, **21**, **23**, **24**, **28** and **29**; in the case of *O. cumana* they are **19** and **24**; while the best for *O. crenata* are **22** and **25**.

In conclusion, the hypothesis on which this work was based has been verified. New strigolactone analogs based on natural products were synthesized and the method to obtain the strigolactones is much more efficient than isolation from plant material, which requires thousands of plants to obtain several micrograms of strigolactones such as strigol or sorgolactone.[12] Our method allows the synthesis of strigolactones with global yields up to 8%, the starting material can be isolated on a multigram scale and only 3–6 facile steps are required. The new compounds stimulate the germination of parasitic weeds and they are very active and convenient for use as leads in preventive herbicides for the honeypot strategy. The achievement of high activity profiles at the lowest concentrations affirmed that only small doses of compounds would be required in herbicide formulations. Compounds with different stereochemical features to the natural strigolactones showed better activity profiles in some cases than those with the same stereochemistry. Thus, structural features must be considered to select the best candidates for each parasitic species tested.

SUPPORTING INFORMATION DESCRIPTION

Supporting Information Available: [^{1}H and ^{13}CNMR of synthesized compounds]. This material is available free of charge via Internet at http://pubs.acs.org

AUTHOR INFORMATION

Corresponding Author

*E–mail: famacias@uca.es. Tel: +34–95–6016370.

Funding

All simulations were performed using computational facilities from 'Servicio de Supercomputación of Área de Sistemas de Información' of the University of Cádiz.

This research was supported by the 'Ministerio de Economía, Industria y Competitividad' (MINEICO), Spain, Project AGL2017-88-083-R.

F.J.R.M. thanks the University of Cádiz for predoctoral support under grant 2018-009/PU/EPIF-FPI-CT/CP.

Notes

The authors declare no competing financial interest.

REFERENCES

(1) Le Corre, V.; Reibel, C.; Gibot-Leclerc, S. Development of Microsatellite Markers in the Branched Broomrape *Phelipanche Ramosa* L. (Pomel) and Evidence for Host-Associated Genetic Divergence. *Int. J. Mol. Sci.* **2014**, 15 (1), 994–1002. https://doi.org/10.3390/ijms15010994.

(2) Yang, C.; Xu, L.; Zhang, N.; Islam, F.; Song, W.; Hu, L.; Liu, D.; Xie, X.; Zhou, W. iTRAQ-Based Proteomics of Sunflower Cultivars Differing in Resistance to Parasitic Weed *Orobanche Cumana*. *Proteomics* **2017**, 17 (13–14), 1–51. https://doi.org/10.1002/pmic.201700009.

(3) Rubiales, D.; Fernández Aparicio, M. Innovations in Parasitic Weeds Management in Legume Crops. A Review. *Agron. Sustain. Dev.* **2012**, 32 (2), 433–439. https://doi.org/10.1007/s13593-011-0045-x.

(4) Macías, F. A.; García-Díaz, M. D.; Pérez-De-Luque, A.; Rubiales, D.; Galindo, J. C. G. New Chemical Clues for Broomrape-Sunflower Host - Parasite Interactions: Synthesis of Guaianestrigolactones. *J. Agric. Food Chem.* **2009**, 57 (13), 5853–5864. https://doi.org/10.1021/jf900870j.

(5) Brookes, G.; Taheripour, F.; Tyner, W. E. The Contribution of Glyphosate to Agriculture and Potential Impact of Restrictions on Use at the Global Level. *GM Crop. Food* **2017**, 8 (4), 216–228. https://doi.org/10.1080/21645698.2017.1390637.

(6) Cimmino, A.; Masi, M.; Rubiales, D.; Evidente, A.; Fernández-Aparicio, M. Allelopathy for Parasitic Plant Management. *Nat. Prod. Commun*. **2018**, 13 (3), 289–294. https://doi.org/10.1177/1934578x1801300307.

(7) Xu, J.; Smith, S.; Smith, G.; Wang, W.; Li, Y. Glyphosate Contamination in Grains and Foods: An Overview. *Food Control* **2019**, 106 (June). https://doi.org/10.1016/j.foodcont.2019.106710.

529 (8) Hedin, P. A. New Concepts and Trends in Pesticide Chemistry. *J. Agric. Food Chem.*
530 **1982**, 30 (2), 201–215. https://doi.org/10.1021/jf00110a001.

531 (9) Zwanenburg, B.; Mwakaboko, A. S.; Kannan, C. Suicidal Germination for Parasitic
532 Weed Control. *Pest Manag. Sci.* **2016**, 72 (11), 2016–2025.
533 https://doi.org/10.1002/ps.4222.

534 (10) Besserer, A.; Puech-Pagès, V.; Kiefer, P.; Gomez-Roldan, V.; Jauneau, A.; Roy, S.;
535 Portais, J.-C.; Roux, C.; Bécard, G.; Séjalon-Delmas, N. Strigolactones Stimulate
536 Arbuscular Mycorrhizal Fungi by Activating Mitochondria. *PLoS Biol* **2006**, 4 (7), e226.

537 (11) Cardoso, C.; Ruyter-Spira, C.; Bouwmeester, H. J. Strigolactones and Root Infestation
538 by Plant-Parasitic *Striga*, *Orobanche* and *Phelipanche* Spp. *Plant Sci.* **2011**, 180 (3), 414–
539 420. https://doi.org/10.1016/j.plantsci.2010.11.007.

540 (12) Humphrey, A. J.; Galster, A. M.; Beale, M. H. Strigolactones in Chemical Ecology:
541 Waste Products or Vital Allelochemicals? *Nat. Prod. Rep.* **2006**, 23 (4), 592–614.
542 https://doi.org/10.1039/b512776a.

543 (13) Lachia, M.; Wolf, H. C.; De Mesmaeker, A. Synthesis of Strigolactones Analogues by
544 Intramolecular [2+2] Cycloaddition of Ketene-Iminium Salts to Olefins and Their
545 Activity on *Orobanche Cumana* Seeds. *Bioorganic Med. Chem. Lett.* **2014**, 24 (9), 2123–
546 2128. https://doi.org/10.1016/j.bmcl.2014.03.044.

547 (14) Lombardi, C.; Artuso, E.; Grandi, E.; Lolli, M.; Spirakys, F.; Priola, E.; Prandi, C. Recent
548 Advances in the Synthesis of Analogues of Phytohormones Strigolactones with Ring-
549 Closing Metathesis as a Key Step. *Org. Biomol. Chem.* **2017**, 17 (c), 8218–8231.
550 https://doi.org/10.1039/C7OB01917C.

551 (15) Mwakaboko, A. S.; Zwanenburg, B. Strigolactone Analogues with a D-Ring Modified at
552 C-2. *European J. Org. Chem.* **2016**, (21), 3495–3499.
553 https://doi.org/10.1002/ejoc.201600576.

554 (16) Tanaka, M.; Sugimoto, Y.; Kuse, M.; Takikawa, H. Synthesis of 7-Oxo-5-Deoxystrigol,
555 a 7-Oxygenated Strigolactone Analog. *Biosci. Biotechnol. Biochem.* **2013**, 77 (4), 832–
556 835. https://doi.org/10.1271/bbb.130020.

557 (17) Cala, A.; Molinillo, J. M. G.; Fernández-Aparicio, M.; Ayuso, J.; Álvarez, J. A.; Rubiales,
558 D.; Macías, F. A. Complexation of Sesquiterpene Lactones with Cyclodextrins: Synthesis
559 and Effects on Their Activities on Parasitic Weeds. *Org. Biomol. Chem.* **2017**, 15 (31),
560 6500–6510. https://doi.org/10.1039/c7ob01394a.

561 (18) Pereira, R. G.; Cala, A.; Fernández-Aparicio, M.; Molinillo, J. M.; Boaventura, M. A.;
562 Macías, F. A. Gibberellic and Kaurenoic Hybrid Strigolactone Mimics for Seed
563 Germination of Parasitic Weeds. *Pest Manag. Sci.* **2017**, 73, 2529−2537.

564 (19) Cala, A.; Zorrilla, J. G.; Rial, C.; Molinillo, J. M. G.; Varela, R. M.; Macías, F. A. Easy
565 Access to Alkoxy, Amino, Carbamoyl, Hydroxy, and Thiol Derivatives of Sesquiterpene
566 Lactones and Evaluation of Their Bioactivity on Parasitic Weeds. *J. Agric. Food Chem.*
567 **2019**, 67 (38), 10764–10773. https://doi.org/10.1021/acs.jafc.9b03098.

568 (20) Azarken, R.; Guerra, F. M.; Moreno-Dorado, F. J.; Jorge, Z. D.; Massanet, G. M.
569 Substituent Effects in the Transannular Cyclizations of Germacranes. Synthesis of 6-Epi-
570 Costunolide and Five Natural Steiractinolides. *Tetrahedron* **2008**, 64 (48), 10896–10905.
571 https://doi.org/10.1016/j.tet.2008.09.017.

572 (21) Kraut, L.; Mues, R.; Sim-Sim, M. Sesquiterpene Lactones and 3-Benzylphthalides from
573 *Frullania Muscicola*. *Phytochemistry* **1994**, 37 (5), 1337–1346.

574 (22) Zorrilla, J. G.; Rial, C.; Varela, R. M.; Molinillo, J. M. G.; Macías, F. A. Facile Synthesis
575 of Anhydrojudaicin and 11,13-Dehydroanhydrojudaicin, Two Eudesmanolide-Skeleton
576 Lactones with Potential Allelopathic Activity. *Phytochem. Lett.* **2019**, 31 (February),
577 229–236. https://doi.org/10.1016/j.phytol.2019.04.014.

578 (23) Gonzalez Collado, I.; Gomez Madero, J.; Martinez Massanet, G.; Rodriguez Luis, F.
579 Partial Synthesis of Sesquiterpene Lactones: A Route to 7,11-Ene-13-
580 Hydroxyeudesmanolides. *J. Org. Chem.* **1991**, 56 (11), 3587–3591.
581 https://doi.org/10.1021/jo00011a025.

582 (24) Cala, A.; Ghooray, K.; Fernández-Aparicio, M.; Molinillo, J. M.; Galindo, J. C.;
583 Rubiales, D.; Macías, F. A. Phthalimide-Derived Strigolactone Mimics as Germinating
584 Agents for Seeds of Parasitic Weeds. *Pest Manag. Sci.* **2016**, 72 (11), 2069–2081.
585 https://doi.org/10.1002/ps.4323.

586 (25) Wavrin, L.; Viala, J. Clean and Efficient Oxidation of Homoallylic and Homopropargylic
587 Alcohols into β,γ-Unsaturated Aldehydes by the Dess-Martin Periodinane. *Synthesis*
588 **2002**, 6 (3), 326–330. https://doi.org/10.1055/s-2002-20029.

589 (26) Malik, H.; Rutjes, F. P. J. T.; Zwanenburg, B. A New Efficient Synthesis of GR24 and
590 Dimethyl A-Ring Analogues, Germinating Agents for Seeds of the Parasitic Weeds
591 *Striga* and *Orobanche* Spp. *Tetrahedron* **2010**, 66 (35), 7198–7203.
592 https://doi.org/10.1016/j.tet.2010.06.072.

593 (27) Rial, C.; Gómez, E.; Varela, R. M.; Molinillo, J. M. G.; Macías, F. A. Ecological
594 Relevance of the Major Allelochemicals in *Lycopersicon Esculentum* Roots and
595 Exudates. *J. Agric. Food Chem.* **2018**, 66 (18), 4638–4644.
596 https://doi.org/10.1021/acs.jafc.8b01501.

597 (28) Matusova, R.; Rani, K.; Verstappen, F. W. A.; Franssen, M. C. R.; Beale, M. H.;
598 Bouwmeester, H. J. The Strigolactone Germination Stimulants of the Plant-Parasitic
599 *Striga* and *Orobanche* Spp. Are Derived from the Carotenoid Pathway. *Plant Physiol.*
600 **2005**, 139 (October), 920–934. https://doi.org/10.1104/pp.105.061382.920.

Figure Captions

Figure 1. Natural strigolactone strigol and synthetic strigolactone GR24, the latter is commonly used as a positive control in bioassays as racemate.

Figure 2. (a) Synthetic procedure to obtain eudesmanestrigolactones (EDSLs, **18**–**26**) from costunolide (**1**). (b) Structure of synthetized EDSLs. (c) Synthetic procedure to obtain dihydroguaianestrigolactones (dihydro-GELs, **27**, **28**) and ester dimer (**29**).

Figure 3. NOE effects observed to confirm the 11*Z* configuration of EDSLs **18**, **19** and **22**, C-11*R* orientation of **26** and 17*Z* configuration of **29**.

Figure 4. (a) Experimental and theoretical ECD spectra of EDSLs **18**–**22** and **23**–**26**. (b) Experimental and theoretical ECD spectra of dihydroguaianestrigolactones **27** and **28**.

Figure 5. Results of parasitic weed bioassay for compounds **18**–**29** and the positive control GR24. Values with statistical significance have been included for most active compounds. For each concentration in the broomrape bioassay, * indicates differences of each compound compared with the negative control (1% v/v acetone in water), as assessed by Dunnett's test at the 0.05 level.

Figure 6. Left, sample of *O. cumana* with application of **25** at 10^{-4} M at the end of the bioassay, where germinated seeds were not observed. Right, sample of *O. cumana* with application of **25** at 10^{-5} M, where more than 90% of germinated seeds were observed.

619 Figures and artwork

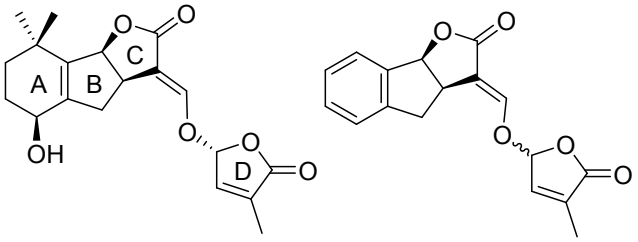

620 (+)-Strigol GR24

621 **Figure 1**

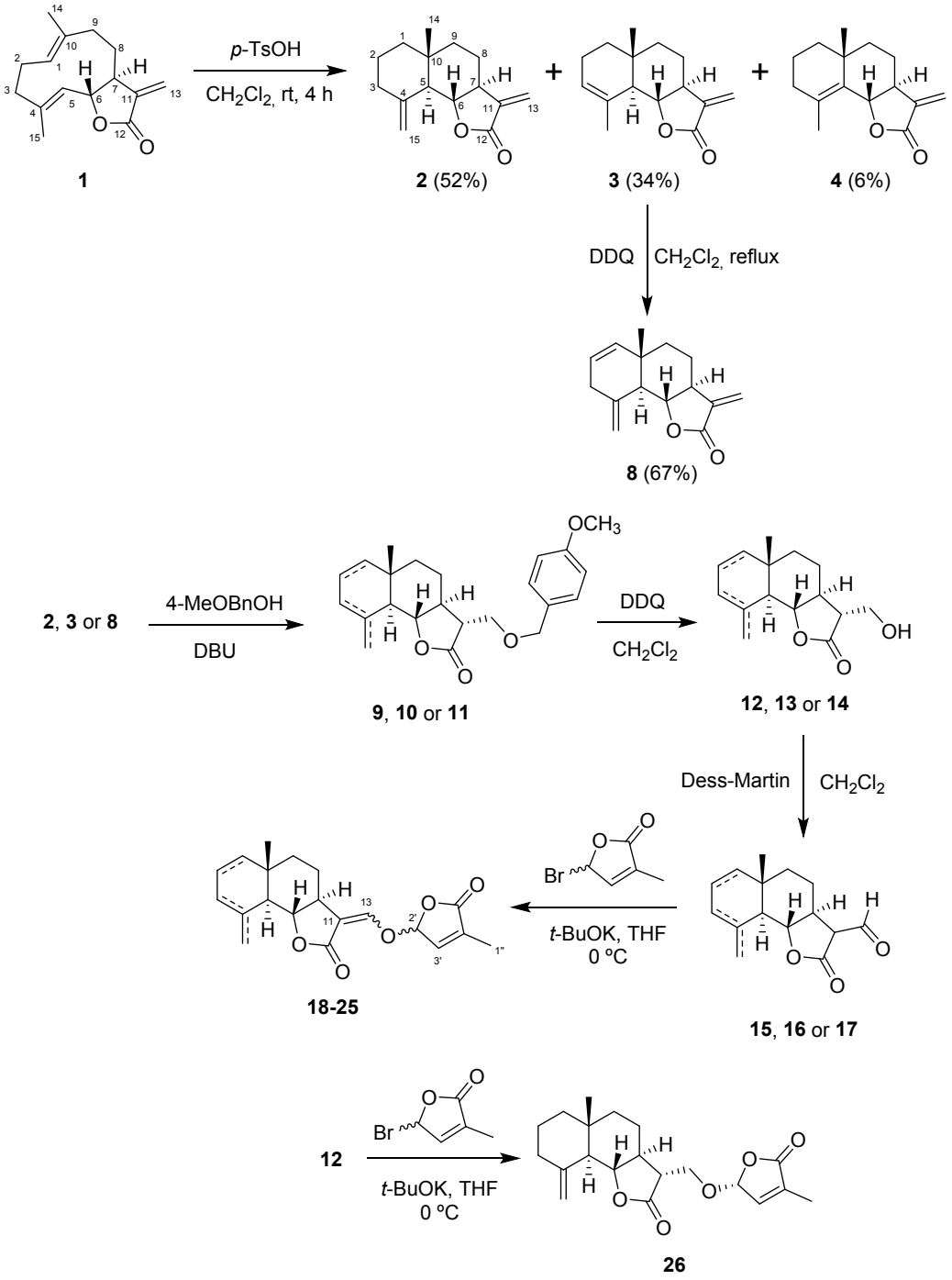

$\Delta^{4,15}$	**2**, **9**, **12**, **15**, **18** (11*Z*, C-2'*R*), **19** (11*Z*, C-2'*S*), **20** (11*E*, C-2'*R*), **21** (11*E*, C-2'*S*)
$\Delta^{3,4}$	**3**, **10**, **13**, **16**, **22** (11*Z*, C-2'*R*+*S*), **23** (11*E*, C-2'*R*)
$\Delta^{1,2}$, $\Delta^{4,15}$	**8**, **11**, **14**, **17**, **24** (11*Z*, C-2'*R*), **25** (11*E*, C-2'*R*)

Figure 2 (a)

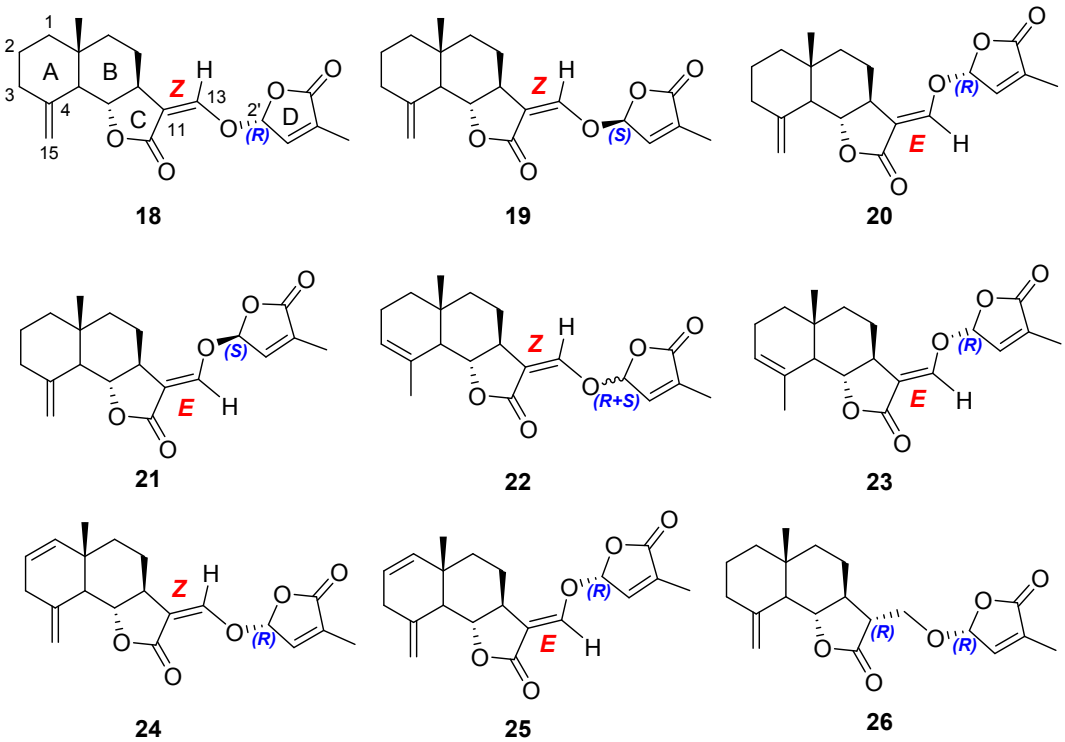

624
625

Figure 2 (b)

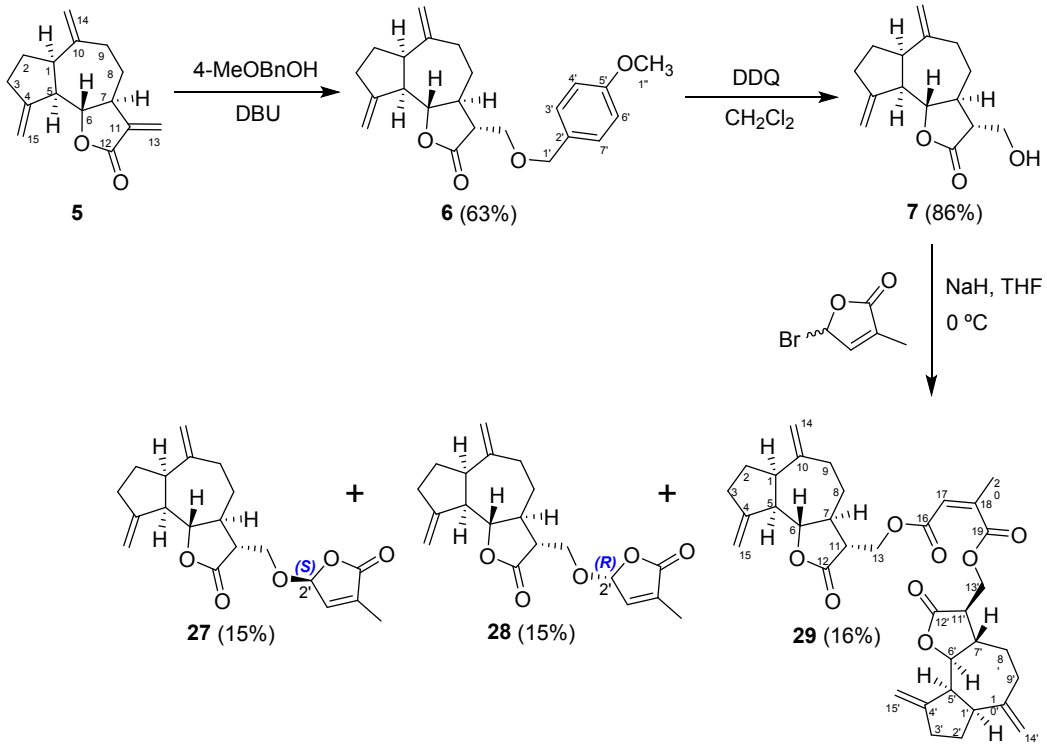

627

628 **Figure 2 (c)**

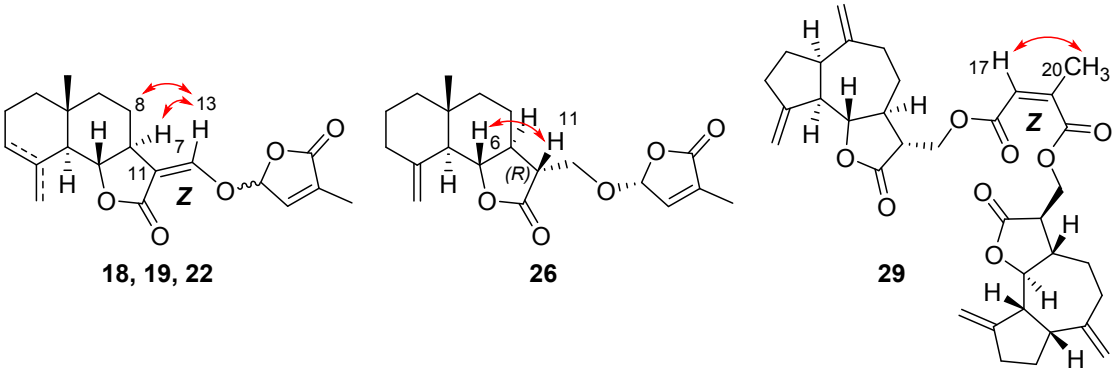

629

630 **Figure 3**

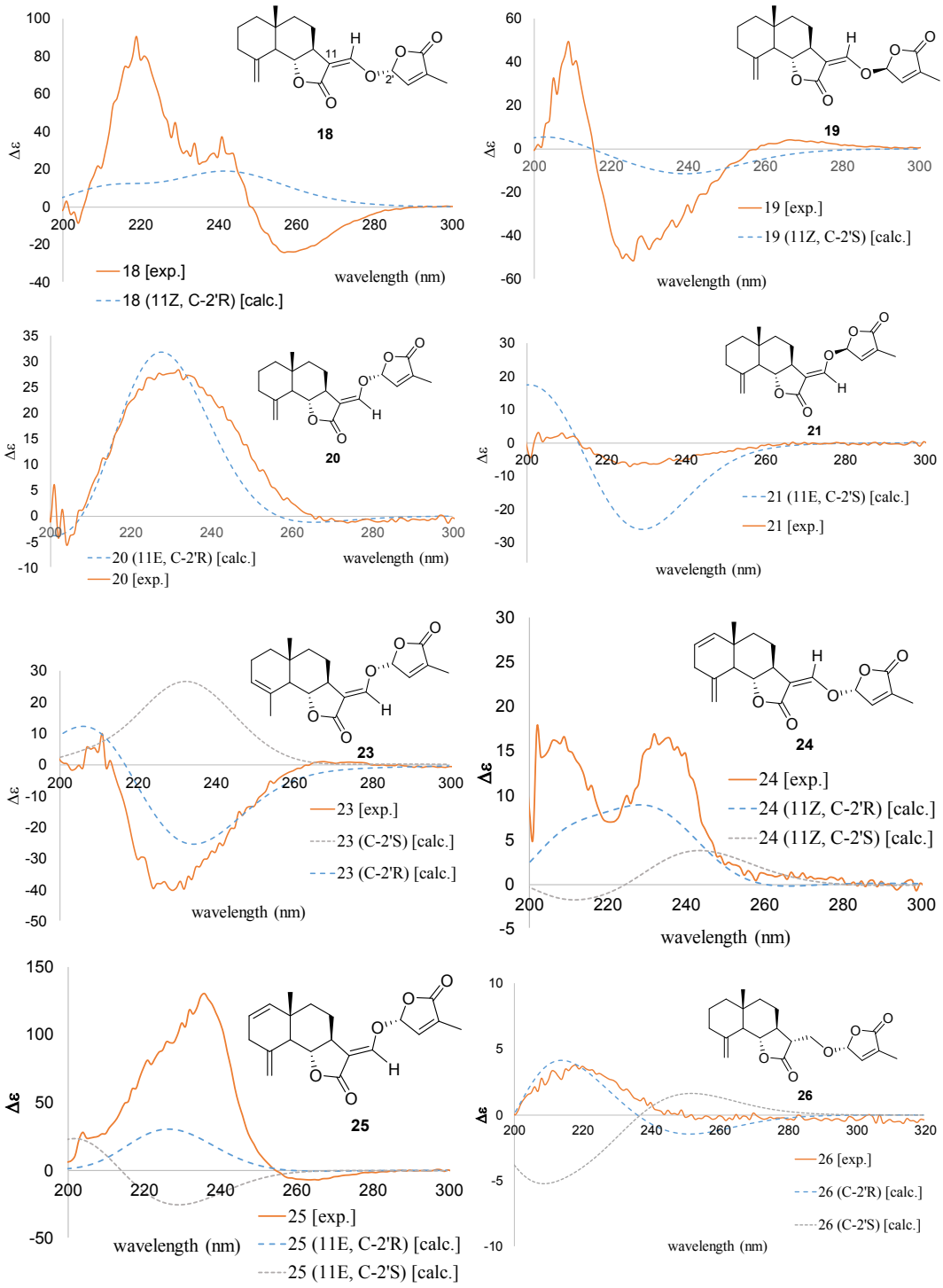

631

632 **Figure 4 (a)**

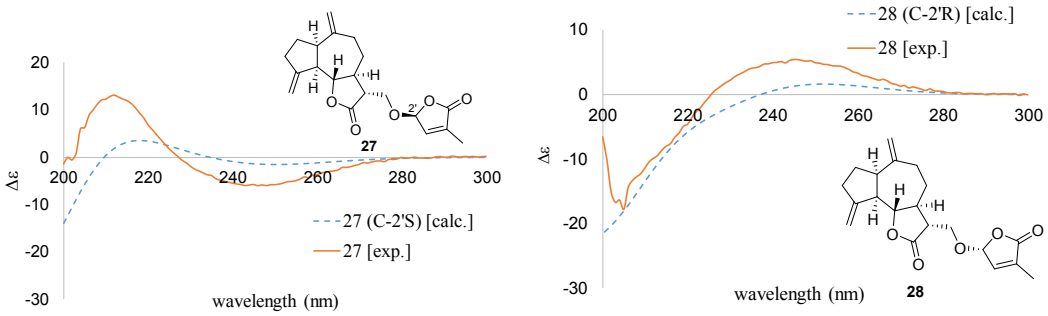

633

634 **Figure 4 (b)**

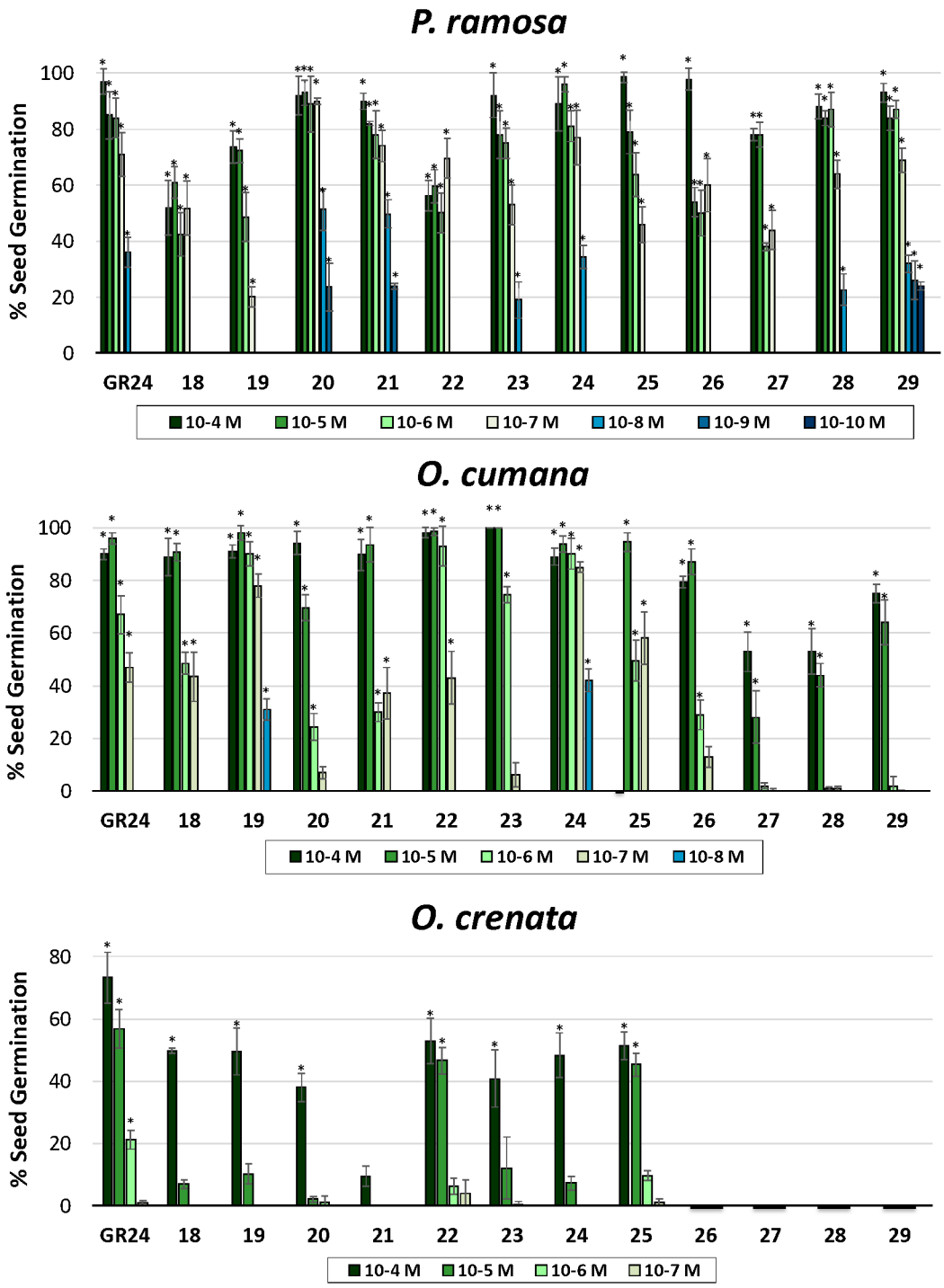

635
636

Figure 5

637

638 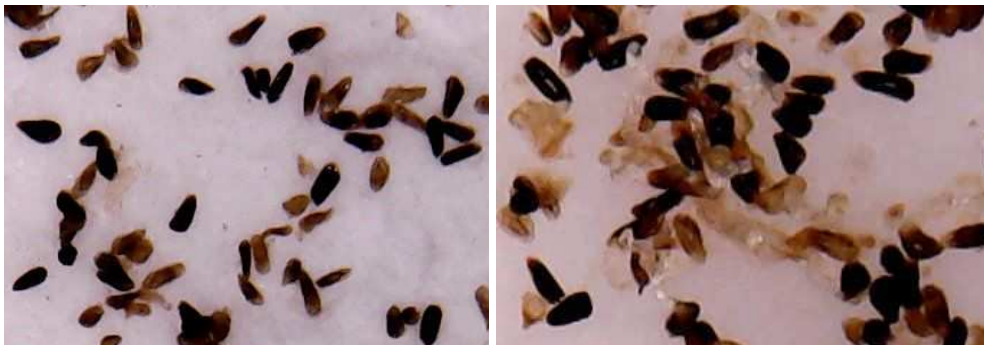

639 **Figure 6**

640 **Table 1.** EC_{50} values of compounds **18**–**29** in M. Only those compounds with activities higher
641 than 50% and active at more than one concentration were analyzed for their EC_{50} (< or >: value
642 out of tested range, n.a.: not active, *: value at which the inhibitory or stimulatory activity was
643 approximately 50%).

	O. crenata	*O. cumana*	*P. ramosa*
	EC_{50} (M)	EC_{50} (M)	EC_{50} (M)
18	10^{-4}*	$9.33 \cdot 10^{-7}$	$<10^{-7}$
19	10^{-4}*	$2.41 \cdot 10^{-8}$	$8.03 \cdot 10^{-7}$
20	$>10^{-4}$	$3.94 \cdot 10^{-6}$	$8.98 \cdot 10^{-9}$
21	n.a.	$2.22 \cdot 10^{-6}$	$8.91 \cdot 10^{-9}$
22	10^{-4}*	$1.24 \cdot 10^{-7}$	$<10^{-7}$
23	$>10^{-4}$	$4.48 \cdot 10^{-7}$	$8.43 \cdot 10^{-8}$
24	$>10^{-4}$	$1.21 \cdot 10^{-8}$	$2.90 \cdot 10^{-8}$
25	10^{-4}*	$1.10 \cdot 10^{-6}$	$1.38 \cdot 10^{-7}$
26	n.a.	$1.91 \cdot 10^{-6}$	$1.65 \cdot 10^{-5}$
27	n.a.	10^{-4}*	$1.78 \cdot 10^{-6}$
28	n.a.	10^{-4}*	$5.27 \cdot 10^{-8}$
29	n.a.	$<10^{-6}$	$3.70 \cdot 10^{-8}$
GR24	$5.77 \cdot 10^{-6}$	$1.34 \cdot 10^{-7}$	$2.27 \cdot 10^{-8}$

644

645

646 **GRAPHIC FOR TABLE OF CONTENTS**

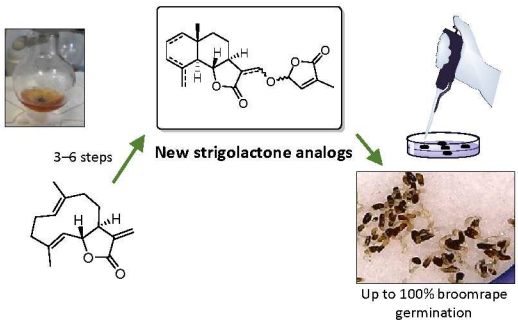

647

648 For Table of Contents Only